

Turret location impact on global performance of a thruster-assisted turret-moored FPSO

S.W. Kim, M.H. Kim* and H.Y. Kang

Department of Ocean Engineering, Texas A&M University, USA

(Received July 15, 2016, Revised August 22, 2016, Accepted August 28, 2016)

Abstract. The change of the global performance of a turret-moored FPSO (Floating Production Storage Offloading) with DP (Dynamic Positioning) control is simulated, analyzed, and compared for two different internal turret location cases; bow and midship. Both collinear and non-collinear 100-yr GOM (Gulf of Mexico) storm environments and three cases (mooring-only, with DP position control, with DP position+heading control) are considered. The horizontal trajectory, 6DOF (degree of freedom) motions, fairlead mooring and riser tension, and fuel consumptions are compared. The PID (Proportional-Integral-Derivative) controller based on LQR (linear quadratic regulator) theory and the thrust-allocation algorithm which is based on the penalty optimization theory are implemented in the fully-coupled time-domain hull-mooring-riser-DP simulation program. Both in collinear and non-collinear 100-yr WWC (wind-wave-current) environments, the advantage of mid-ship turret is demonstrated by the significant reduction in heave at the turret location due to the minimal coupling with pitch mode, which is beneficial to mooring and riser design. However, in the non-collinear WWC environment, the mid-turret case exhibits unfavorable weathervaning characteristics, which can be reduced by employing DP position and heading controls as demonstrated in the present case studies. The present study also reveals the plausible cause of the failure of mid-turret Gryphon Alpha FPSO in milder environment than its survival condition.

Keywords: hull-mooring-riser-DP coupled simulation program; turret-moored FPSO; collinear and non-collinear wind-wave-current; bow turret; midship turret; DP heading control; penalty method; weathervane; mooring tension; riser tension; fuel consumption; Gryphon Alpha FPSO

1. Introduction

For the past two decades, the internal turret mooring FPSO is a dominant paradigm for FPSO development. The turret system has a bearing that permits FPSOs to rotate freely so that the heading of the vessel can be towards the direction of minimal environmental force. The FPSO turret location is an important factor for topsides design and overall system dynamics. The system dynamics and performance are related to the turret location. As the turret location approaches the bow part of the vessel, the weathervaning capability is generally improved, but the vertical motion at its location can significantly increase due to coupling with pitch motion. This increased vertical motion is a concern for riser design. Particularly when SCRs (steel catenary risers) are used, large amplitude downward motion at turret can cause serious structural problem for risers. If the turret is

*Corresponding author, Professor, E-mail: m-kim3@tamu.edu

located in the mid part of the vessel, the vertical motion can be minimized with less pitch-induced contribution, which is beneficial for mooring-riser design. The disadvantage of the midship turret location is that it generally increases yaw motions, and thus heading control is more difficult. A thruster-assisted system can overcome the disadvantage of the midship turret.

Considering those pros and cons, the Gryphon Alpha FPSO was developed to have a mid-ship internal turret with a thruster-assisted positioning system in the North Sea. Unfortunately, during a storm event milder than the survival condition, its stationkeeping system failed and risers and mooring lines were damaged. It occurred in February 2011 from 175 miles north east of Aberdeen under the wind speed 60 knots and the significant wave height about 12 meters. The FPSO lost its heading control and faced environmental loads from beam side. In consequence, the anchors and mooring lines were damaged. Figure 1 shows the anchor chain failure. (Finucane 2012).

The Gryphon Alpha FPSO originally equipped ten mooring lines connected to the mid-ship turret, as shown in Fig. 2, and it was assisted by five thrusters. The thruster-assisted system was responsible for heading control. When it was shut-down during the incident, mooring lines could not bear unexpectedly larger environmental loadings from the beam side. Fig. 2 presents the initial stage of the Gryphon Alpha FPSO drive off incident. The Gryphon Alpha FPSO initially maintained the heading towards the wind direction.



Fig. 1 The Anchor Chain Failure of Gryphon Alpha FPSO (Finucane 2012)

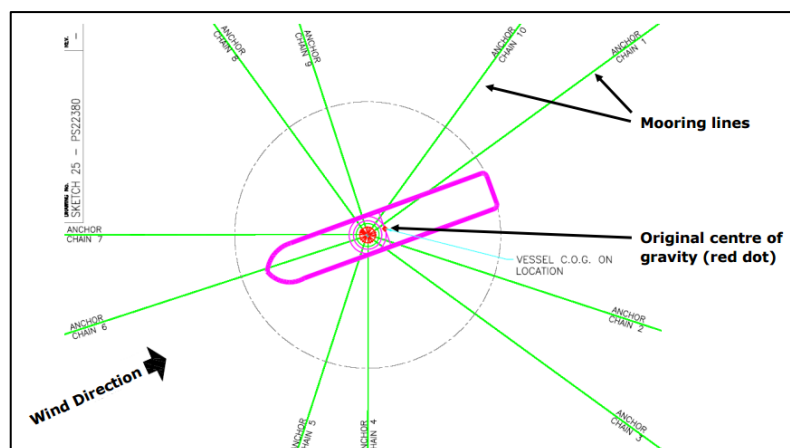


Fig. 2 The Initial Stage of the Gryphon (Finucane 2012)

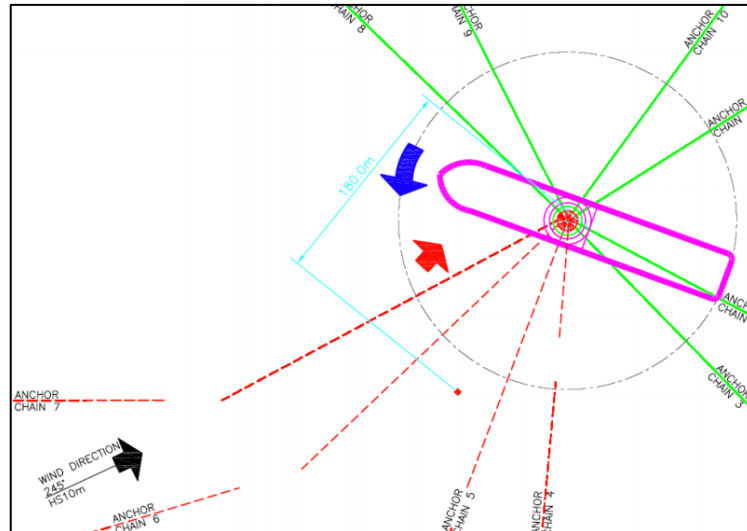


Fig. 3 The Final Stage of the Gryphon Alpha FPSO (Finucane 2012)

Fig. 3 presents the final stage of the Gryphon Alpha FPSO incident. Four mooringlines and four anchor chains were broken. The FPSO drifted off 180 m in a sway direction.

This kind of circumstance needs to be checked during the design stage. However, the fully coupled hull-mooring-riser-thruster analysis tool in time domain is rare. The authors have developed such a simulation program in time domain, and it is used here to investigate the global performance of a turret-moored FPSO with thruster-assisted control.

Thiagarajan and Finch (1999) conducted wave basin tests to evaluate the global motion change due to four different turret locations; external, internal bow, internal mid, and internal stern. They found that the lowest vertical motion occurred when the turret was near midship or LCG (Longitudinal Center of Gravity). The stern internal turret location was very poor in the vertical motion performance. Duggal *et al.* (2000) conducted a numerical analysis and wave basin model test to design an FPSO having an internal turret mooring system for the eastern sea of Canada 100-yr storm condition. According to the conclusions of this study, the mid-ship turret considerably enhanced the vertical-motion capability compared to that of the bow-turret case. However, the equilibrium heading angle of the mid-ship turret was significantly increased compared to that of the bow-turret case. This phenomenon also degraded the horizontal stability of the FPSO.

Kannah and Natarjan (2006) analyzed the global performance of an FPSO with varying internal turret locations by experiments. They tested three internal turret locations, i.e. bow, mid-ship, and semi-aft locations, with several ballast conditions under sinusoidal waves coming from head sea. According to their results, the heave RAO of the bow location is smaller than that of the mid-ship turret condition, which contradicts with other researches including the present paper.

This paper aims to analyze the global dynamic performance of a turret-moored FPSO with thrusters for two internal turret positions. Both collinear and non-collinear 100-yr storm conditions are considered. The 6DOF FPSO motions and mooring tensions with and without thrusters are compared. When thrusters are employed, the cases of position control only and position+heading

control are also compared. The fuel consumptions of the corresponding thruster-assisted cases are also compared. The DP simulation method including fuel-consumption estimation is detailed in Kim (2016).

2. Simulation model description

The thruster-assisted FPSO has a 200,000 ton tanker moored in 1,829 m water depth. Hull, mooring, riser, and thruster coupled time-domain simulations were conducted based on CHARM3D program (e.g., Yang and Kim 2011, Kang and Kim 2014) developed by the research group of 2nd author during the past 20 years. The thruster-assisted system simulation and thruster allocation using a penalty method is based on Kim (2016). The wind and current forces for different headings are based on the OCIMF (Oil Companies International Maritime Forum) data. The wave forces are calculated for many heading angles with 5-degree interval (Tahar and Kim 2003). The second-order slowly varying wave forces and vessel responses are based on the Newman's approximation, which has been validated through comparisons with experimental results (e.g., Kim *et al.* 2005). The wave forces and hydrodynamic coefficients of the hull are calculated from 3D diffraction/radiation panel program WAMIT. The panel discretization used for the present FPSO is illustrated in Figs. 4(a), 4(b) and 5. The hull viscous damping is included through the modified Morison formula representing cross-flow drags with an equivalent projected area. Regarding the wind spectrum, the API (America Petroleum Institute) wind spectrum was used to generate the dynamic wind forces.

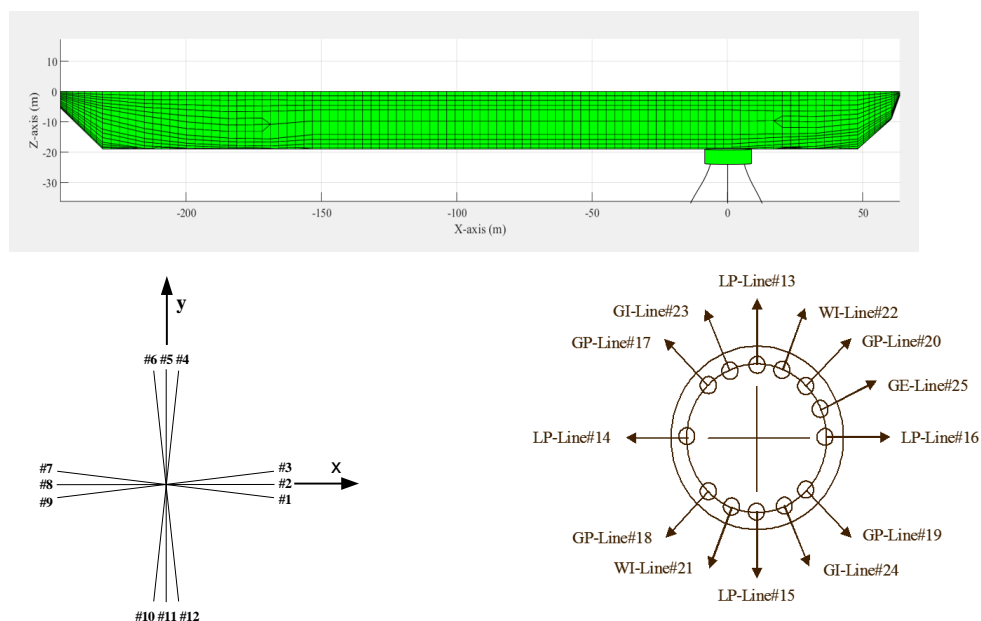


Fig. 4 (a) Bow Turret Case Mesh Model and Mooring-Riser Arrangement

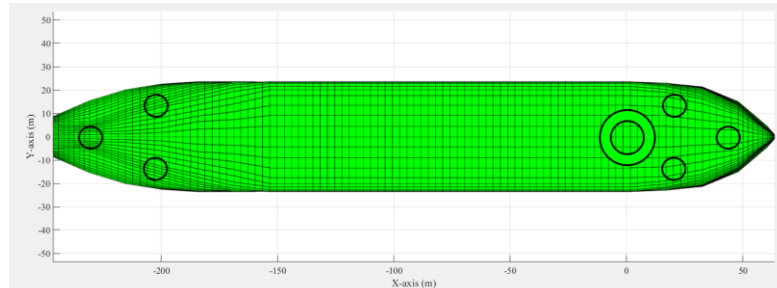


Fig. 4 (b) Bow Turret, Thrusters, and Riser Configuration

Table 1 Principal Particulars of FPSO Vessel

Designation	Symbol	Unit	Quantity
Production rate		bpd	120,000
Storage		bbls	1,440,000
Vessel size		kDWT	200
Length b/w perpendiculars	Lpp	<i>m</i>	310
Breadth	B	<i>m</i>	47.2
Depth	H	<i>m</i>	28.0
Draft	T	<i>m</i>	18.9
Length to beam ratio	L/B		6.57
Beam to draft ratio	B/T		2.5
Displacement	Δ	ton	240,869
Block coefficient	Cb		0.85
Center of buoyancy forward section 10	FB	<i>m</i>	6.6
Water plane area	A	<i>m</i> ²	13,400
Water plane coefficient	Cw		0.9164
Center of water plane area forward section 10	FA	<i>m</i>	1.0
Center of gravity above base	KG	<i>m</i>	13.3
Metacentric height transverse	MGt	<i>m</i>	5.8
Metacentric height longitudinal	MGl	<i>m</i>	403.8
Trans. radius of gyration in air	Kxx	<i>m</i>	14.8
Long. radius of gyration in air	Kyy	<i>m</i>	77.5
Yaw radius of gyration	Kzz	<i>m</i>	79.3
Wind area front	Af	<i>m</i> ²	1012
Wind area side	Ab	<i>m</i> ²	3772
Turret in centerline behind Fpp (20.5% Lpp)		<i>m</i>	63.5
Turret elev. below tanker base		<i>m</i>	1.5
Turret diameter		<i>m</i>	15.8

Table 2 Mooring Line Particulars

Designation	Unit	Quantity
Water depth	<i>m</i>	1,829
Pre-tension	<i>kN</i>	1,424
Number of lines		4 × 3
Degree between the 3 lines	<i>deg.</i>	5
Length of mooring line	<i>m</i>	2,652
Radius of location of chain stoppers on turn table	<i>m</i>	7.0
<i>Segment 1: Chain</i>		
Length at anchor point	<i>m</i>	121.9
Diameter	<i>cm</i>	9.52
Dry weight	<i>N/m</i>	1,856
Weight in water	<i>N/m</i>	1,615
Stiffness AE	<i>kN</i>	912,120
<i>Segment 2: Polyester</i>		
Length	<i>m</i>	2,438
Diameter	<i>cm</i>	16.0
Dry weight	<i>N/m</i>	168.7
Weight in water	<i>N/m</i>	44.1
Stiffness AE	<i>kN</i>	186,800
<i>Segment 3: Chain</i>		
Length at anchor point	<i>m</i>	91.4
Diameter	<i>cm</i>	9.53
Dry weight	<i>N/m</i>	1,856
Weight in water	<i>N/m</i>	1,615
Stiffness AE	<i>kN</i>	912,120

Table 3 Riser Particulars

Riser Type	Top Tension	OD	AE	EI	Weight Dry/Wet	Cdn
	<i>kN</i>	<i>cm</i>	<i>kN</i>	<i>kNm²</i>	<i>N/m</i>	
Liquid Production (LP)	2224	44.5	1.83 × 10 ⁷	276	1927 1036	1
Gas Production (GP)	1223	38.6	1.08 × 10 ⁷	113	1708 525	1
Water Injection (WI)	4048	53.1	1.86 × 10 ⁷	224	2802 1897	1.414
Gas Injection (GI)	2714	28.7	3.14 × 10 ⁶	64	1810 1168	1.414
Gas Export (GE)	912	34.3	8.63 × 10 ⁶	71	1357 423	1
Total Length of Risers		3657.4 m				

Table 4 Thruster Characteristics and Constraints

Thruster Maximum Capacity	150 KN
Thruster Maximum Change Rate	20 KN /sec
Thruster Angle Change Rate	10 deg / sec
Thruster Position (A.P=0, C.L=0)	T1(290 m,0 m), T2(275 m,-15m), T3(275 m,15 m) T4(35 m,-15 m) T5(35 m,15 m) T6(20 m,0 m)
Thruster Capacity Constraint (KN)	$0 < T_{1,2,3,4,5,6} < 150$
Thruster Angle Constraint (deg)	$0 < \alpha_{1,2,3,4,5,6} < 360$
Thruster Rate Constraint Rate (KN/sec)	$0 < \dot{T}_{1,2,3,4,5,6} < 20$
Thruster Angle Change Rate (deg/sec)	$0 < \dot{\alpha}_{1,2,3,4,5,6} < 20$
Required Force Constraint	$\tau = Bu$

Table 5 Principal Particulars of the Bow and Mid-Ship Turret Cases depending on turret locations

Designation	Symbol	Unit	BOW	MID
Trans. radius of gyration in air	Kxx	<i>m</i>	14.8	14.2
Long. radius of gyration in air	Kyy	<i>m</i>	77.5	134.3
Yaw radius of gyration	Kzz	<i>m</i>	79.3	135.3
Turret in centerline behind Fp (Turret Position)		<i>m</i>	63.5	155

The bow and mid turret locations of the FPSO are 63.5 m and 155 m behind FPP. The coordinate origin is located at the center of turret and MWL (mean water level). The positive x is toward head and z-axis is positive upward. The change of principal particulars due to different turret locations is presented in Table 5.

Twelve chain-polyester-chain mooring lines and thirteen SCRs are applied in the simulation. The mooring and riser elements are modeled by high-order FEM (finite element method; Ran and Kim 1997). Six azimuth thrusters were implemented in the simulation for both bow and mid-turret cases. The hull mesh with the inner-bow-turret and mooring, thrusters, and riser arrangement are, for example, shown in Figs. 4(a) and 4(b).

The extended Kalman Filter, the PID controller based on LQR theory, the penalty-method-based thruster allocation were integrated in the thruster-assisted controller. The PID gain was calculated to minimize energy inputs, and the thrust allocation is based on the penalty method to minimize the fuel consumption.

The required forces and moments that can keep the position of an FPSO can be defined by multiplying the PID gains and error matrix. The key function of a PID controller design is to define the gain control. In PID controller design, the system is assumed as linear time invariant

system. The equations of motion of the linear time-invariant system (Ryu 2003) is given by in Eq. (1)

$$\dot{\mathbf{x}} = \mathbf{A}\mathbf{x} + \mathbf{B}\mathbf{u}, \mathbf{y} = \mathbf{C}\mathbf{x} + \mathbf{v} \quad (1)$$

Where, dot ($\dot{\cdot}$) denotes time derivative, and each vector written in lower case can be described by the following set of definitions

$$\text{State } \mathbf{x} = [u, x, v, y, \omega, \psi]^T \quad \text{Control Input } \mathbf{u} = [\tau_x, \tau_y, \tau_\phi]^T \quad \text{Measurement } \mathbf{y} = [x, y, \psi]^T$$

$$\text{Measurement-Noise } \mathbf{v} = [v_x, v_y, v_\psi]^T$$

Where,

$$\mathbf{A} = \mathbf{M}^{-1} \begin{bmatrix} 0 & 0 & 0 & 0 & 0 & 0 \\ 1 & 0 & 0 & 0 & 0 & 0 \\ 0 & 0 & 0 & 0 & 0 & 0 \\ 0 & 0 & 1 & 0 & 0 & 0 \\ 0 & 0 & 0 & 0 & 0 & 0 \\ 0 & 0 & 0 & 0 & 1 & 0 \end{bmatrix} \quad \mathbf{B} = \mathbf{E} = \mathbf{M}^{-1} \begin{bmatrix} 1 & 0 & 0 \\ 0 & 0 & 0 \\ 0 & 1 & 0 \\ 0 & 0 & 0 \\ 0 & 0 & 1 \\ 0 & 0 & 0 \end{bmatrix} \quad \mathbf{C} = \begin{bmatrix} 0 & 1 & 0 & 0 & 0 & 0 \\ 0 & 0 & 0 & 1 & 0 & 0 \\ 0 & 0 & 0 & 0 & 0 & 1 \end{bmatrix} \quad \mathbf{M} = \begin{bmatrix} M_{11} & 0 & 0 & 0 & 0 & 0 \\ 0 & 1 & 0 & 0 & 0 & 0 \\ 0 & 0 & M_{22} & 0 & M_{26} & 0 \\ 0 & 0 & 0 & 1 & 0 & 0 \\ 0 & 0 & M_{62} & 0 & M_{66} & 0 \\ 0 & 0 & 0 & 0 & 0 & 1 \end{bmatrix}$$

Where,

$M_{11} = m + a_{11}(0)$ $M_{22} = m + a_{22}(0)$ $M_{26} = m + a_{26}(0)$ $M_{62} = m + a_{62}(0)$ $M_{66} = I + a_{66}(0)$, m is the mass of the floating structure, I is the moment of inertia in z-direction, and $a_{ij}(0)$ is added masses at zero frequency, and $\hat{\mathbf{x}}$ is the state estimation vector .

In thrust allocation module, the penalty method showed the best fuel consumption performance (Kim 2016). According to the turret locations, the moment arms of thrusters are different. Therefore, those factors are considered in the required force and moment constraints of the optimization problem.

Object to

$$\min \left(\frac{1}{2} \mathbf{x}^T \mathbf{H} \mathbf{x} + \frac{1}{2} \mathbf{u}^T \mathbf{K} \mathbf{u} + c \left(\begin{array}{l} \max\{0, \mathbf{u} - \mathbf{u}_{\max}\}^2 + \max\{0, \mathbf{u}_{\min} - \mathbf{u}\}^2 \\ + \max\{0, \frac{\mathbf{u}_{\text{previous}} - \mathbf{u}_{\text{current}}}{dt} - \dot{\mathbf{u}}_{\max}\}^2 + (\mathbf{R}\mathbf{F} - \mathbf{B}\mathbf{u})^2 \end{array} \right) \right) \quad (2)$$

$$\text{where } \mathbf{x} = (x, y, \phi, u, v, r)^T \quad \mathbf{u} = (T_1 \cos \alpha, T_1 \sin \alpha, \dots, T_n \cos \alpha, T_n \sin \alpha)^T$$

\mathbf{H} : State weight matrix

\mathbf{K} : Fuel consumption parameter weight matrix

$\mathbf{R}\mathbf{F}$: Required force & moment matrix (3×1)

\mathbf{B} : Thrust allocation matrix (3×n)

\mathbf{u} : Thruster matrix (n×1)

$\mathbf{u}_{\min}, \mathbf{u}_{\max}$: Thrust constraint

$\dot{\mathbf{u}}_{\max}$: Thrust rate constraint

Where,

$$\mathbf{R}\mathbf{F} = \begin{bmatrix} X \\ Y \\ N \end{bmatrix} = \begin{bmatrix} T_{x1} \cos \alpha_1 + T_{x2} \cos \alpha_2 + \dots + T_{xn} \cos \alpha_n \\ T_{y1} \sin \alpha_1 + T_{y2} \sin \alpha_2 + \dots + T_{yn} \sin \alpha_n \\ y_1 T_{x1} \cos \alpha_1 - x_1 T_{y1} \sin \alpha_1 + y_2 T_{x2} \cos \alpha_2 - x_2 T_{y2} \sin \alpha_2 + \dots + y_n T_{xn} \cos \alpha_n - x_n T_{yn} \sin \alpha_n \end{bmatrix}$$

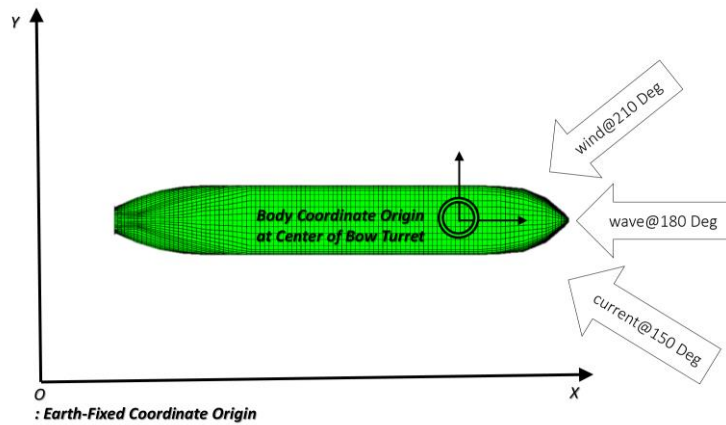


Fig. 5 Non-collinear Environmental Loads Configuration

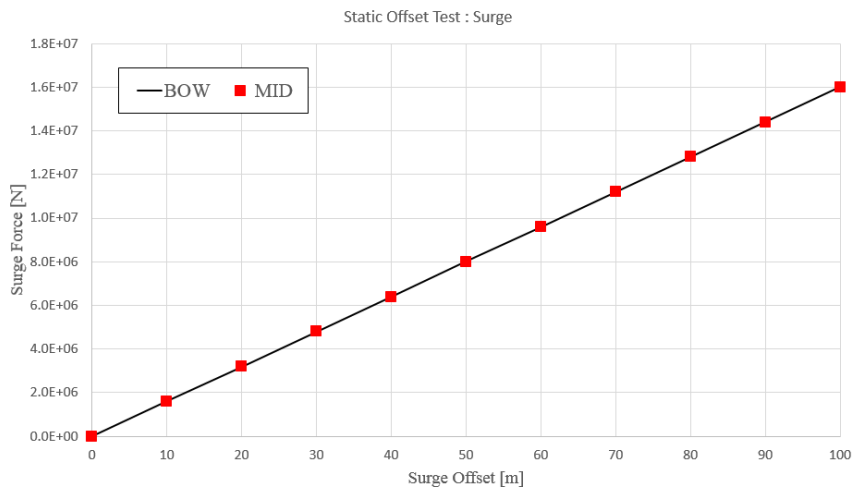


Fig. 6 Static Offset Test

For illustration, survival environmental conditions are considered. First, GOM 100-yr collinear WWC (wind= 41.1 m/s at 10 m; wave= Jonswap spectrum with $H_s=12.19$ m, $T_p=14$ s, enhancement parameter=2.5; current=1.07 m/s at MWL) condition from the head of the FPSO was conducted. Then, GOM 100-yr non-collinear case (Fig. 5) was performed to show the differences in motions and thruster characteristics under the similarly harsh but more spread environmental condition.

The static-offset simulation was conducted to compare the surge stiffness of the mooring system depending on turret locations. It is seen as expected that the surge mooring stiffness is not affected due to the turret position. The P gain of the dynamic positioning system is defined as 800 KN based on these static test results.

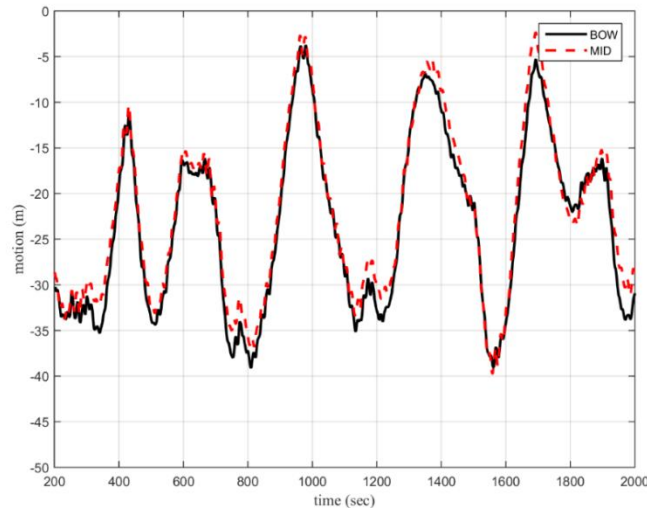


Fig. 7 Surge Motion Time Series of GOM 100-yr Collinear Environment (mooring only case)

3. Numerical results and discussions

In the following, the FPSO motions and mooring fairlead tensions are compared for two different turret locations. The origin for the response for the two cases is located at the respective turret locations.

- 100-yr Collinear-WWC-Case Simulation Results

The GOM 100-yr storm collinear condition was simulated first without any thrusters. As expected, the surge response, shown in Fig. 7, is dominated by slowly-varying motions and the two turret locations produce almost the same surge time histories. This suggests that the turret location has negligible effect on surge motion.

The heave motion, however, shows significant difference between the two cases. The heave amplitude of the mid-ship is significantly (70%) decreased because there is little pitch-induced heave motion. In the bow-turret case, the contribution from the pitch-induced heave is much greater than the pure heave, as can be seen in Fig. 8.

In case of the midship turret, the total heave is small since pitch-induced-heave is negligible. The pure heave motion is also small in this case because the heave RAO itself calculated from WAMIT is small near the peak of the input wave spectrum. For double checking, the heave RAO is regenerated from the time series of the mid-turret case by using the square root of the ratio of the heave-response spectrum to the incident wave spectrum. It agrees very well with WAMIT-calculated RAO as shown in Fig. 9. If we remove the pitch-induced contribution, the bow turret case also exhibits a similar trend as shown in Fig. 9.

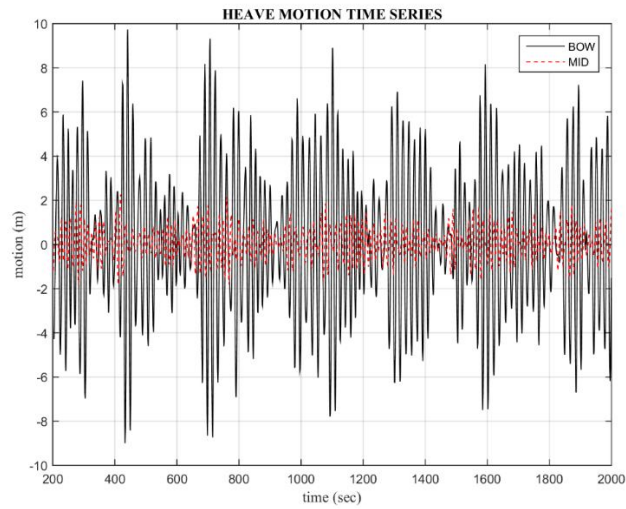


Fig. 8 Heave Motion Time Series of GOM 100-yr Collinear Environment

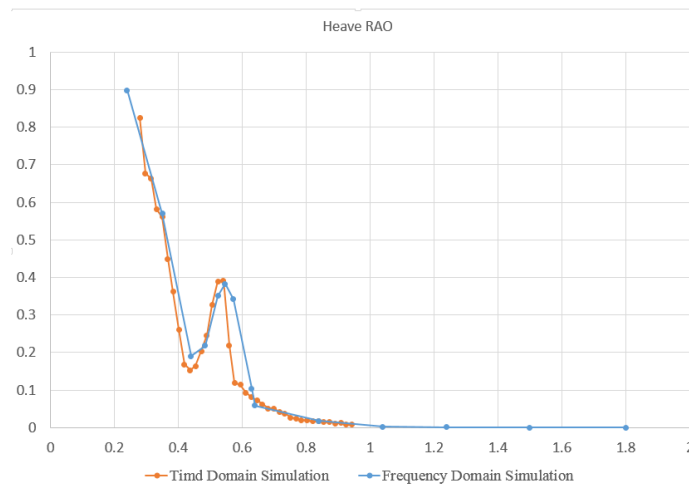


Fig. 9 Heave RAO Comparison

The pitch-motion time series are presented in Fig. 10. As expected, the pitch amplitude is not sensitive to the turret location. Although there exist small differences in the pattern of the time series, when their spectra are compared, they are almost the same.

Fig. 11(a) presents the mooring top-tension time histories of the mid- and bow-turret cases. The mooring line considered is the #2 taut-side line. The maximum tensions for the bow and mid-turret cases are 3,210 KN and 3,060 KN. In the mid-turret case, the high frequency tension part is greatly reduced compared to the bow-turret case due to much smaller heave motions. In case of riser which is the #22 water injection line, the maximum tensions of the bow- and mid-turret cases are

8,800 KN and 4,600KN. The maximum value of the mid-ship turret is about 52% of the bow-turret case. The vertical motion reduction is the main reason of this tendency. Large downward heave motions are very critical for the design of SCRs since it can cause temporal local dynamic buckling near the touch-down point (Eom *et al.* 2014, Kim and Kim 2015). So, with regard to the mooring and riser design, the mid-turret location could be seen as an attractive design, which was the main motivation of the Gryphon Alpha FPSO mid-turret design. Then, the next question is “Do we have the same advantage by using mid-turret even in similarly harsh non-collinear environment?” This question is further investigated in the next section.

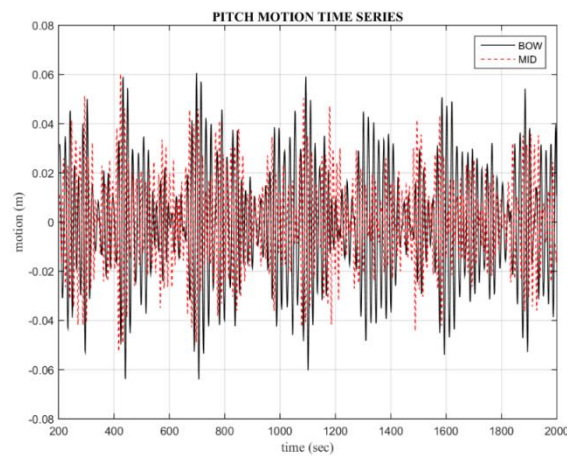


Fig. 10 Pitch Motion Time Series of GOM 100-yr Collinear Environment (mooring only case)

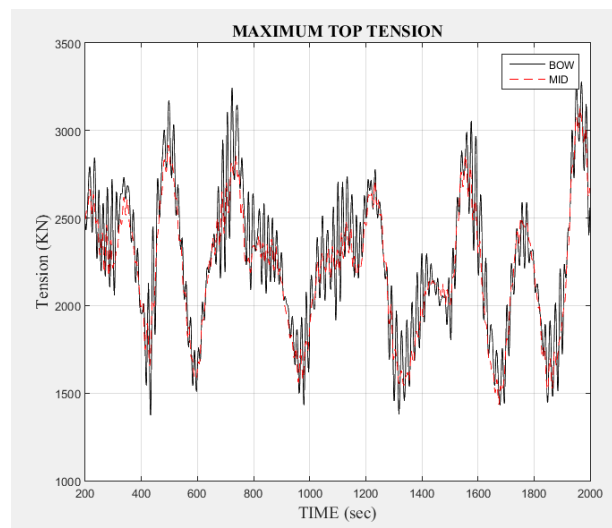


Fig. 11 (a) Mooring Top Tension time histories in GOM 100-yr Collinear Environment (mooring only case)

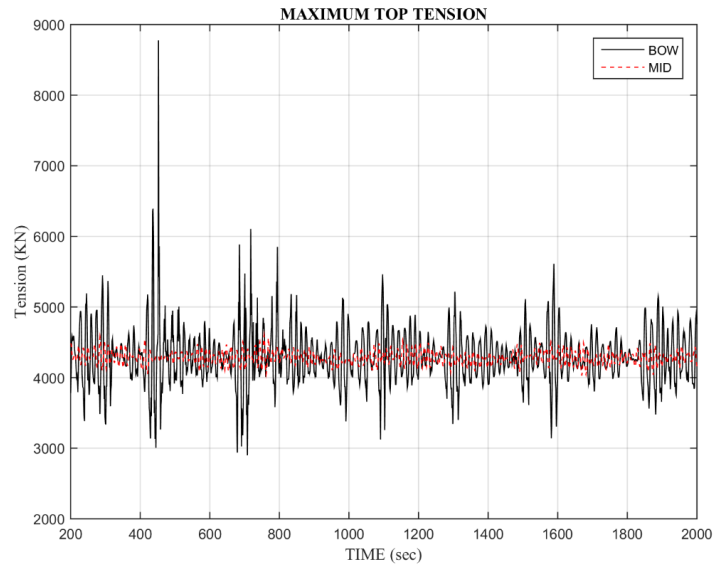


Fig. 11 (b) Riser Top Tension time histories in GOM 100-yr Collinear Environment (mooring only case)

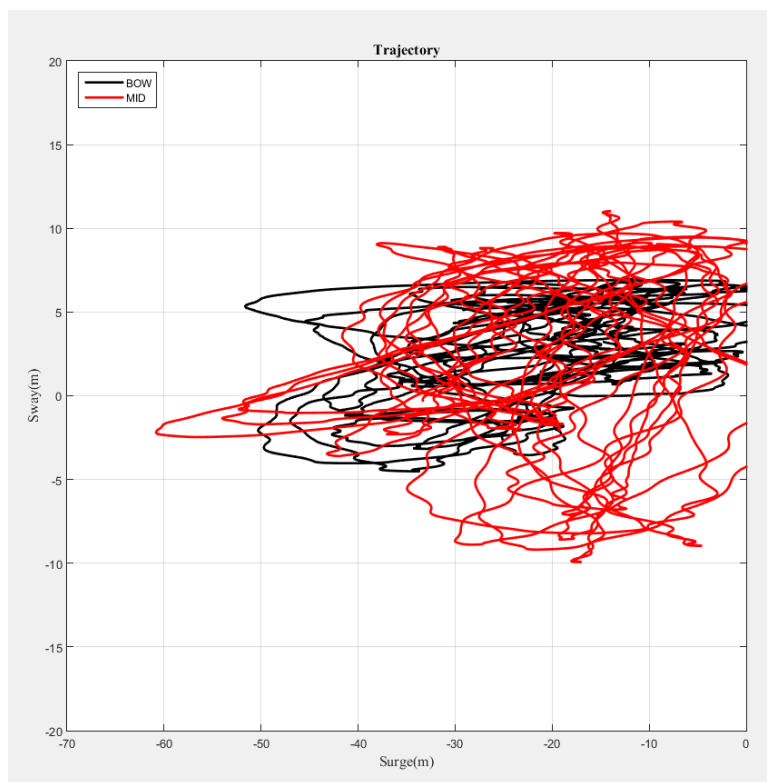


Fig. 12 Surge-Sway Trajectory of the Bow and the Mid-Turret Cases (mooring only case)

- GOM 100-yr Non-collinear WWC & Mooring Only case

In this section, we compare the global performance of the two turret locations in a particular non-collinear WWC condition. Fig. 12 shows the surge-sway trajectory of FPSO without thrust operation. Fig. 13 presents FPSO 6DOF motions. The mid-turret case shows larger excursions in both surge and sway directions compared to the bow-turret case. Particularly, the mid-turret case exhibits large dynamic yaw motions with largely deviated mean yaw angle. It means that the FPSO has to face waves coming with average-40-degree starboard angle. Considering additional slowly-varying yaw responses, the situation can be worse. This phenomenon can cause large variations of WWC loadings i.e. the advantage of weathervaning to minimize the environmental loadings becomes non-effective. So, despite the advantage of smaller vertical motions at the turret, this may be the reason why the mid-turret design is not popular mainly due to the reduced weathervane capability. This may be one of the reasons why the mooring system of the Gryphon FPSO failed even for storms milder than survival condition. On the other hand, the bow turret case is more likely to weathervane to the dominant environmental-loading direction.

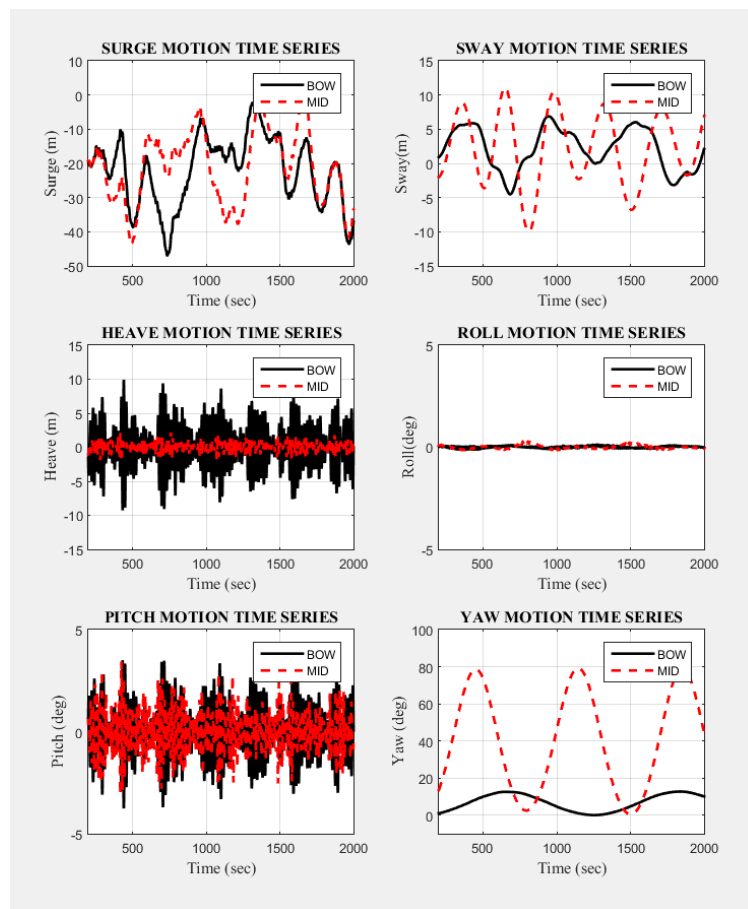


Fig. 13 6DOF Motions of the Bow and Mid-Turret Cases (mooring only case)

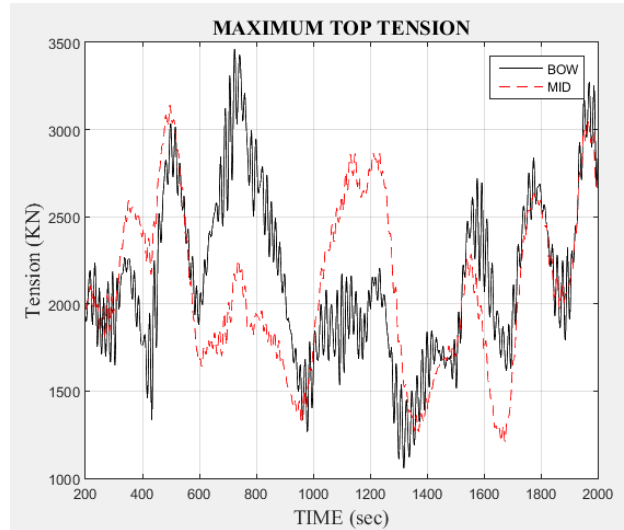


Fig. 14 (a) Mooring Top Tension time histories in GOM 100yr Non-collinear Environment (mooring only case)

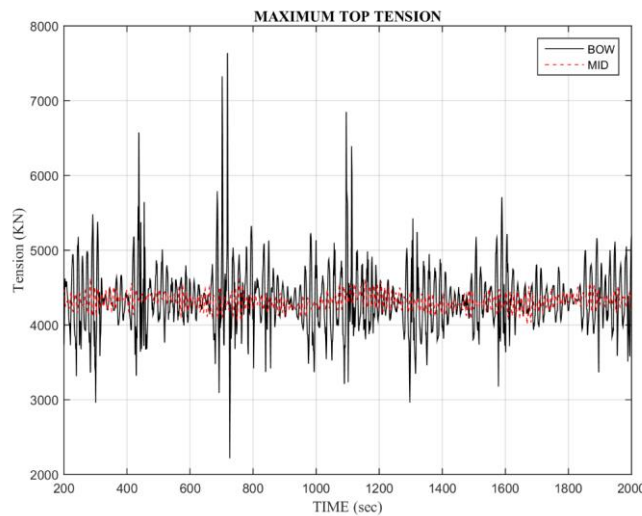


Fig. 14 (b) Riser Top Tension time histories of the Bow and Mid-Turret cases in GOM 100-yr Non-collinear Environment (mooring only case)

Fig. 14 shows the time series of the fairlead mooring tension and riser tension of the bow and mid turret cases under GOM 100-yr non-collinear environment. The reduction of the maximum top tension in the mid-ship turret location is noticeable. Therefore, the advantage of mid-turret location in terms of mooring and riser design is still obvious even in the non-collinear environment except for the critical disadvantage of poorer weathervane capability. The poorer weathervane

capability may be resolved by employing additional thrusters, which is the subject of the next section.

- GOM 100-yr non-collinear WWC with DP position Control (but w/o heading control)

Fig 15 shows the surge and sway trajectory of FPSO under the GOM 100-yr non-collinear environmental condition with the thrusters. For this example, the position control is applied but heading control is not applied. The sway trajectory of the mid-ship turret case is much reduced compared to Fig. 12, but it is still larger than the bow-turret case. The main reason why the sway trajectory is reduced is that the thruster-assisted system counteracts the sway deviation. The dynamic yaw motions are also significantly reduced compared to Fig. 13-yaw. This result implies that the mid-ship turret with thrusters is more practically applicable than without thruster case. Despite the improvement by including the DP position control, the mean yaw angle is still around 40 degrees from the wave direction, which is not a desirable situation. Therefore, additional heading control by thruster-assisted system is needed, as shown in the next section.

Fig. 16 shows the 6DOF motion time histories of the bow and mid-turret cases. The DPS makes the sway excursion smaller by 7 m.

Fig. 17(a) shows the fairlead mooring top tension of the bow and mid-turret cases. Compared to without thruster-assisted system (Fig. 14(a)), the maximum top tension of the bow turret case was reduced from 3,460 KN to 2,940 KN. The maximum tension of the mid-turret case is also reduced from 3,060 KN to 2,960 KN with the thruster-assisted system. According to the result, due to large mean yaw angle in the case of midship turret, sway motions are increased and contribute to slowly varying tensions.

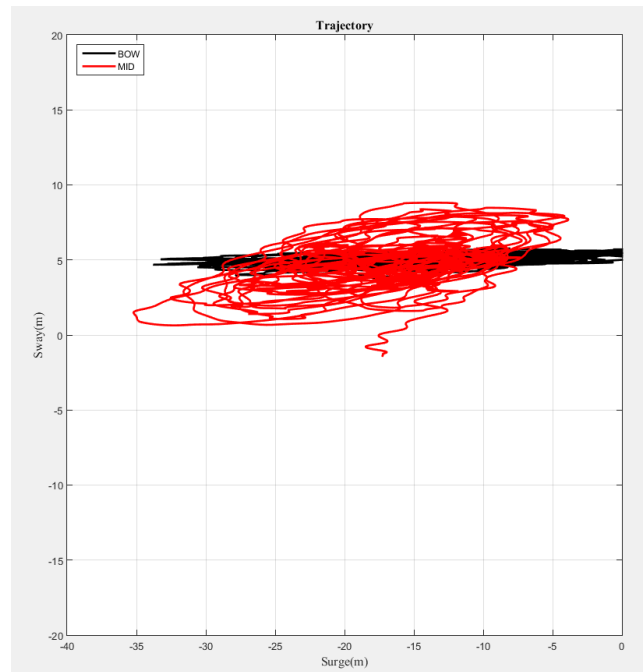


Fig. 15 Surge-Sway Trajectory of the Bow and Mid-Turret Cases (with DP position control)

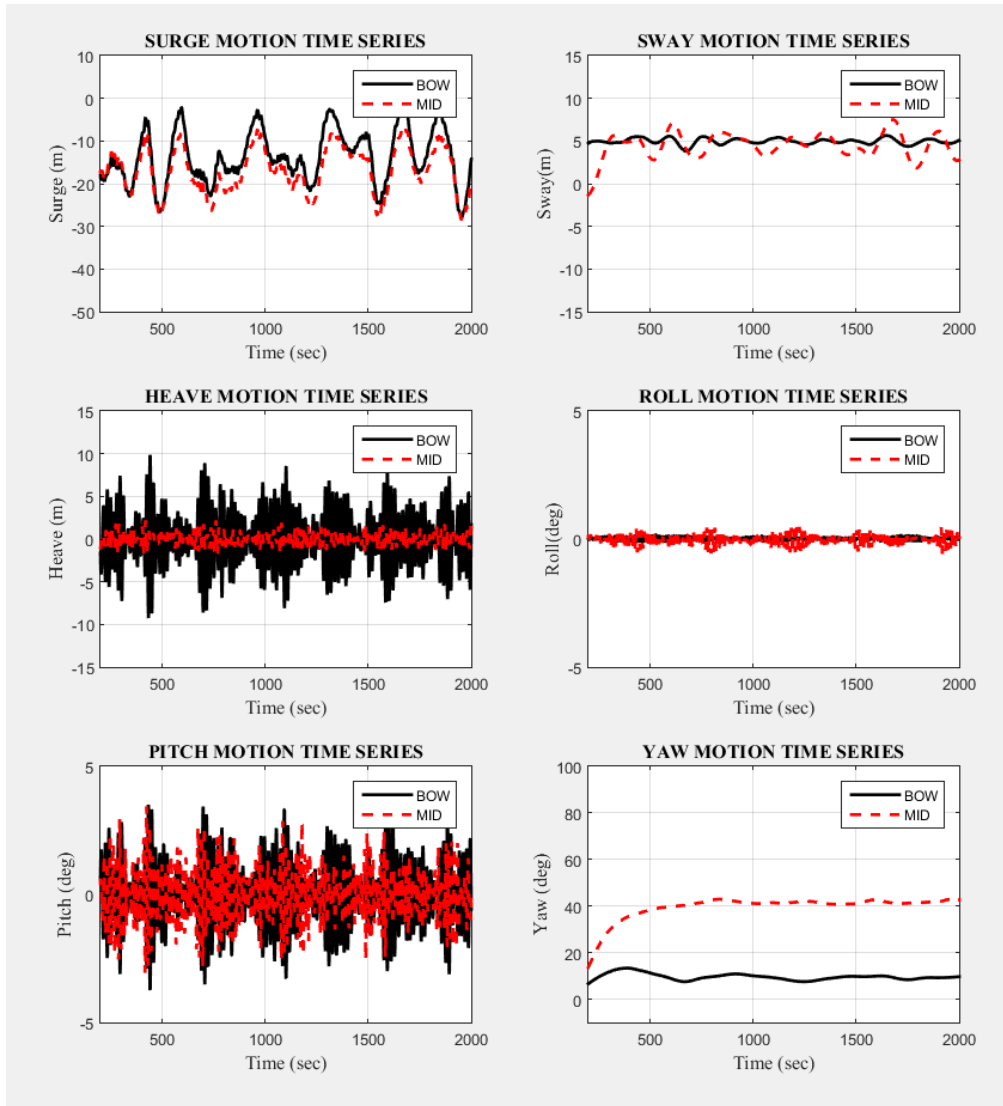


Fig. 16 6DOF Motion Time Series of the Bow and Mid-Turret Cases (with DP position control)

Fig. 17(b) shows the fairlead riser top tension of the bow- and mid-turret cases. Compared to without thruster-assisted system (Fig. 14(b)), the maximum top tension of the bow turret case was decreased from 8,800 KN to 6,200 KN. The maximum tension of the mid-turret case is also reduced from 4,700 KN to 4,500 KN with the DPS.

Fig. 18 shows fuel-consumption time histories depending on turret locations. The fuel consumption formula as a function of required power/thrust is given in Kim (2016). According to the graph, the fuel consumption of the mid-ship turret is appreciably (15%) larger than that of the bow-turret case. Finally, we next consider the same case with additional DP heading control.

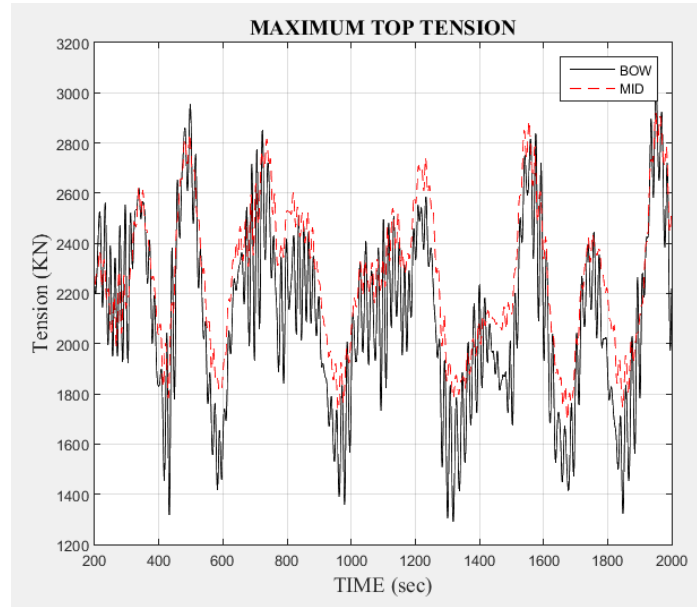


Fig. 17 (a) Mooring Top Tension time histories for the Bow and Mid-Turret Cases (with DP position control)

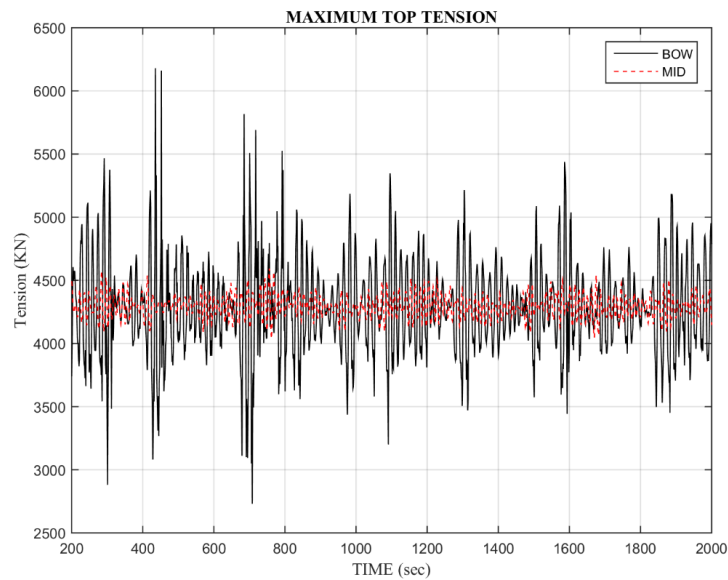


Fig. 17 (b) Riser Top Tension time histories for the Bow and Mid-Turret Cases (with DP position control)

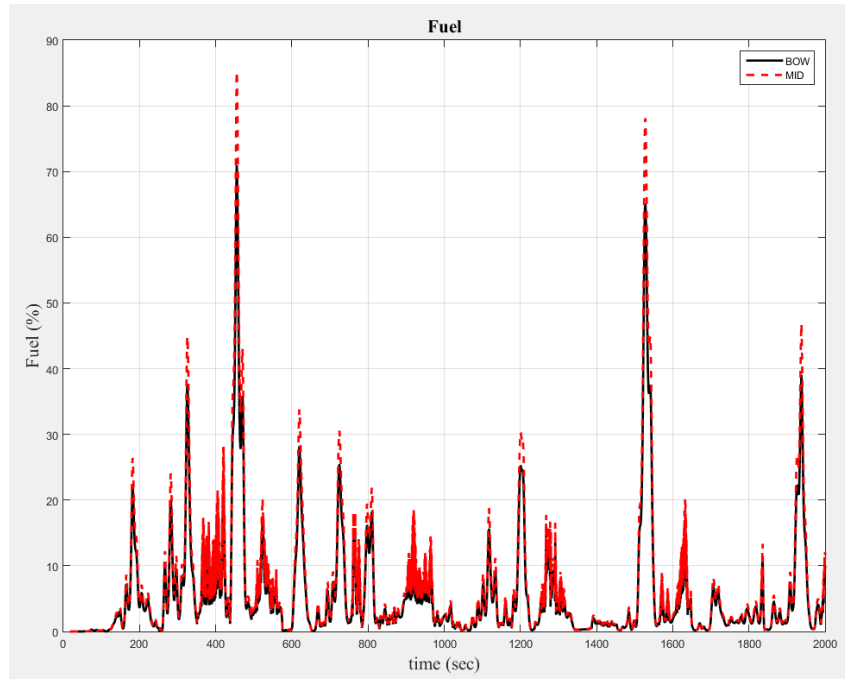


Fig. 18 Fuel Consumption of the Bow and Mid-Turret Cases (with DP position control)

- GOM 100-yr non-collinear WWC with DP location and heading control

Fig. 19 shows the surge and sway trajectory of an FPSO in the GOM 100-yr non-collinear environmental conditions when a thruster-assisted system is doing both position and heading controls. Fig. 20 shows the 6DOF Motion Time Histories of the Bow and Mid-Turret Cases. The target heading direction in this case is zero-degree i.e., parallel to the wave direction. The sway deviations are much reduced (by 5 m) compared to the previous cases. The main reason why the sway trajectory becomes smaller is that the thruster-assisted system maintains the heading close to the wave direction. The mean yaw angle of the mid-turret case is also significantly reduced from about 40 to 10 degrees compared to the DP position control only case. This implies that the mid-turret location can be advantageous to the mooring riser system when DP does both position and heading controls.

Fig. 21(a) shows the corresponding mooring top-tension time histories. The maximum top tension of the bow turret case was reduced from 2,940 kN to 2,590 kN while that of mid-turret case is reduced from 2,960 kN to 2,370 kN with the additional DPS Heading Control. The mooring top tension was appreciably reduced by additionally employing DPS heading control.

Fig. 21(b) shows the corresponding top-tension time histories. The maximum top tension of the bow turret case was reduced from 6,200 kN to 6,130 kN while that of mid-turret case is reduced from 4,500 kN to 4,410 kN with the additional DPS Heading Control.

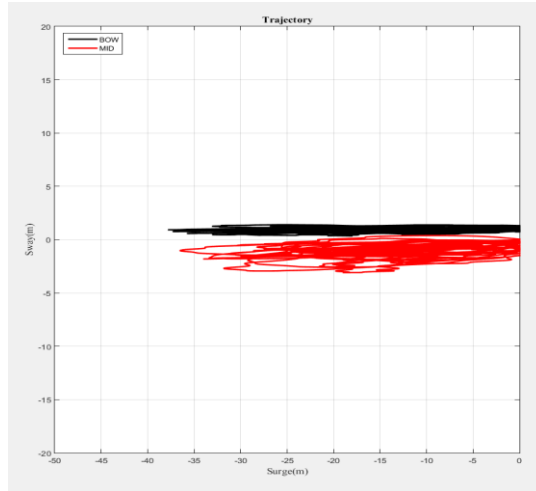


Fig. 19 Surge- Sway in GOM 100-yr Non-collinear Case

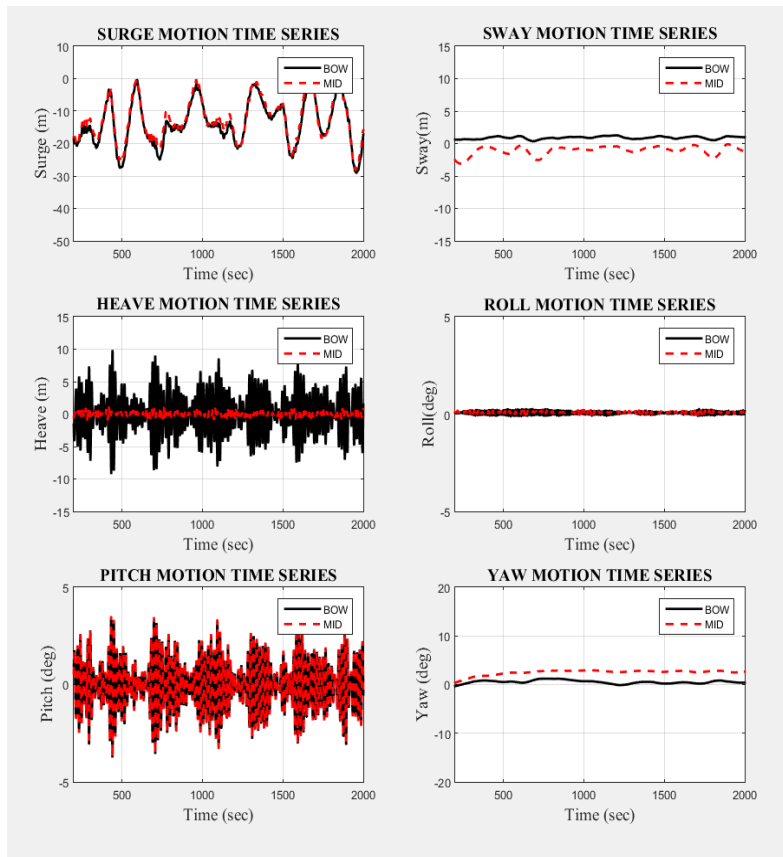


Fig. 20 6DOF motion Time Histories under 100-yr Non-collinear WWC with additional DP Heading Control

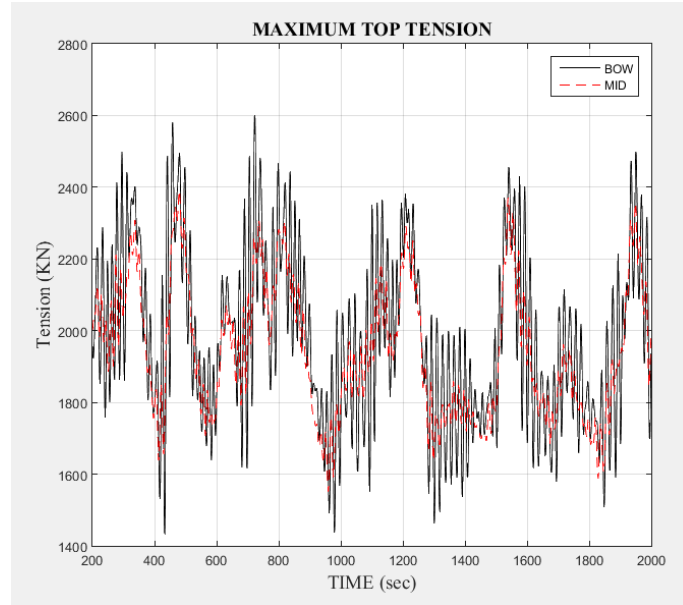


Fig. 21 (a) Mooring Top Tension time histories of the Bow and Mid-Turret cases in GOM 100-yr Non-collinear WWC with additional DP Heading Control

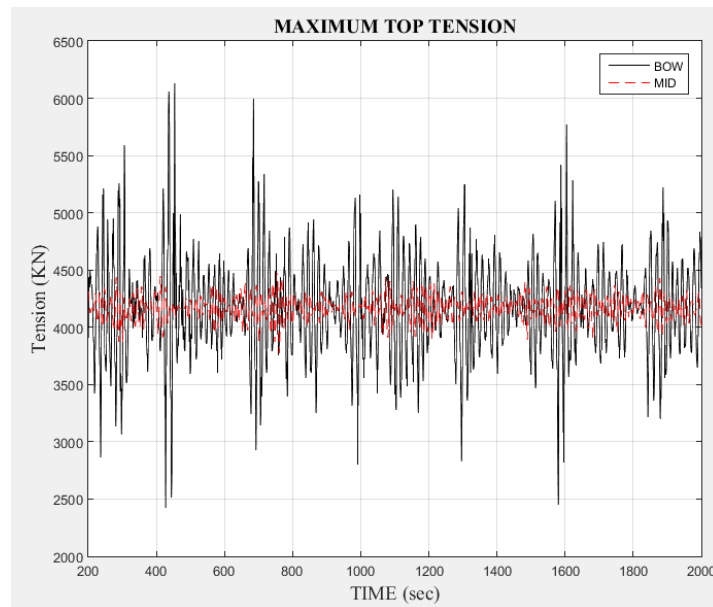


Fig. 21 (b) Riser Top-Tension time histories of the Bow and Mid-Turret cases in GOM 100-yr Non-collinear WWC with additional DP Heading Control

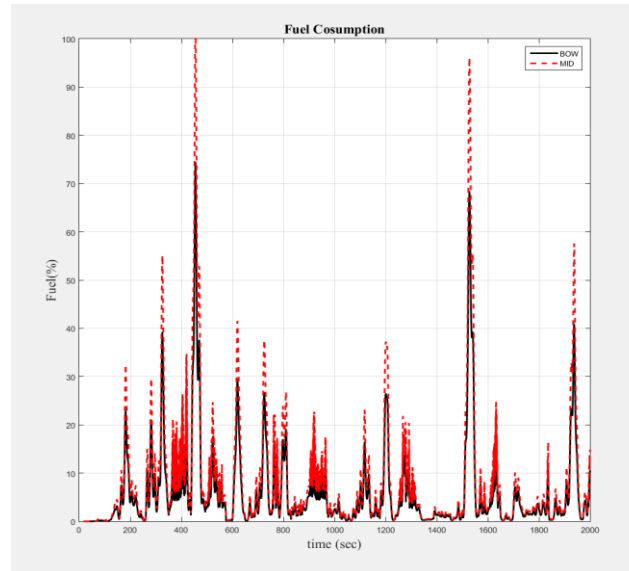


Fig. 22 Fuel Consumption Index under 100-yr Non-collinear WWC with additional DP Heading Control

Finally, Fig. 22 shows the fuel-consumption time histories according to the locations. Compared to the position-control-only case, the accumulated fuel consumption is increased by 5% by employing additional heading control since it requires more thrust forces.

4. Conclusions

The impact of the turret location on the global performance of a turret-moored FPSO with DP control was investigated by comparing two different internal turret location cases: i.e., bow and midship. Both collinear and non-collinear 100-yr GOM storm environments were considered. The horizontal trajectory, 6DOF motions, fairlead mooring tension, and fuel consumptions were calculated and compared. Three cases (mooring-only, with DP position control, with DP position+heading control) were analyzed. The PID controller based on LQR theory and the thrust-allocation algorithm which is based on the penalty optimization theory were implemented in the time-domain hull-motion with DP control simulation program.

In collinear WWC environment, the advantage of mid-ship turret was demonstrated by the significant reduction in heave at the turret location due to the minimal coupling with pitch mode. However, in non-collinear WWC environment, the mid-turret case, despite the same advantage in heave reduction, case exhibited unfavorable position control and weathervaning characteristics. The disadvantage of the mid-turret case, however, can significantly be reduced by employing DP position and heading controls, as demonstrated in the present case studies, while keeping the advantage of much smaller vertical motions and maximum mooring tensions at turret location. The fuel consumption of the DPS is higher in the case of mid-turret.

In conclusion, the mid-turret case is better than the bow-turret case in terms of mooring and riser design but it has to work with proper DP position+heading control. Otherwise, it may have

the risk of weathervaning malfunction in non-collinear environment, which actually happened in the failure of Gryphon Alpha FPSO.

Acknowledgements

This research was partly supported by DSME (Daewoo Shipbuilding and Marine Engineering).

References

- Duggal, A.S., Heyl, C.N. and Vance, G.P. (2000), *Global Analysis of the Terra Nova FPSO Turret Mooring System*, Paper presented at the Offshore Technology Conference.
- Eom, T.S., Kim, M.H., Bae, Y. and Cifuentes, C. (2014), "Local dynamic buckling of FPSO steel catenary riser by coupled time-domain simulations", *Ocean Syst. Eng.*, **4**(3), 215-241.
- Finucane, M. (2012), Details of Gryphon Incident - Lessons Learned *Aberdeen International Organization Safety and Health Conference*.
- Isherwood, R. (1973). Wind resistance of merchant ships. *RINA Supplementary Papers*, 115.
- Kang, H.Y. and Kim, M.H. (2014), "Safety assessment of caisson transport on a floating dock by frequency-and time-domain calculations", *Ocean Syst. Eng.*, **4**(2), 99-115.
- Kannah, T.R. and Natarajan, R. (2006), "Effect of turret location on the dynamic behaviour of an internal turret moored FPSO system", *J. Naval Architect. Marine Eng.*, **3**(1), 23-37.
- Kim, M.H., Koo, B.J., Mercier, R. and Ward, E. (2005), "Vessel/mooring/riser coupled dynamic analysis of a turret-moored FPSO compared with OTRC experiment", *Ocean Eng.*, **32**(14), 1780-1802.
- Kim, S.J. and Kim, M.H. (2015), "Dynamic behaviors of conventional SCR and lazy-wave SCR for FPSOs in deepwater", *Ocean Eng.*, **106**, 396-414.
- OCIMF. (1996), Prediction of wind loads and current loads on VLCCs.
- Ran, Z. and Kim, M.H. (1997), "Nonlinear coupled responses of a tethered spar platform in waves", *Int. J. Offshore Polar Eng.*, **7**(2).
- Rao, S.S. and Rao, S. (2009), *Engineering optimization: theory and practice*: John Wiley & Sons.
- Rindarøy, M. and Johansen, T.A. (2013), "Fuel optimal thrust allocation in dynamic positioning", *IFAC Proceedings Volumes*, **46**(33), 43-48.
- Ryu, S. (2003), *Hull/Mooring/Riser coupled motion simulations of thruster-assisted moored platforms*. Texas A&M University.
- Kim, S.W. (2016), Eco-Friendly Dynamic Positioning Algorithm Development *Texas A&M University Ph.D. Dissertation*.
- Tahar, A. and Kim, M.H. (2003). "Hull/mooring/riser coupled dynamic analysis and sensitivity study of a tanker-based FPSO". *Appl. Ocean Res.*, **25**(6), 367-382.
- Thiagarajan, K. and Finch, S. (1999). "An Investigation Into the Effect of Turret Mooring Location on the Vertical Motions of an FPSO Vessel". *J. Offshore Mech. Arct.*, **121**(2), 71-76.
- Yang, C.K. and Kim, M.H. (2011), "The structural safety assessment of a tie-down system on a tension leg platform during hurricane events", *Ocean Syst. Eng.*, **1**(4), 263-283.